Available online at www.sciencedirect.com
SCIENCE DIRECT
Diamond & Related Materials 15 (2006) 1023–1028
DIAMOND AND RELATED MATERIALS
www.elsevier.com/locate/diamond

# Selective growth of vertically aligned carbon nanofibres in sub-micron patterns and Raman mapping of produced arrays

V.B. Golovko [a,*], M. Cantoro [b], S. Hofmann [b], B. Kleinsorge [b], J. Geng [a], D. Jefferson [a], A.C. Ferrari [b], J. Robertson [b], B.F.G. Johnson [a]

[a] Department of Chemistry, University of Cambridge, Lensfield Road, Cambridge CB2 1EW, UK
[b] Department of Engineering, University of Cambridge, Trumpington Street, Cambridge CB2 1PZ, UK

Available online 17 February 2006

**Abstract**

Carbon nanofibres are grown using a highly purified cobalt colloid catalyst. Nanocontact printing was used to deposit catalyst in patterns with sub-micron resolution over large areas on silicon wafers. Plasma Enhanced Chemical Vapour Deposition allows the direct growth of vertically aligned carbon nanofibres with good surface adhesion at lower temperatures. Production of the catalyst is described. Rutherford back-scattering detection Scanning Electron Microscopy and Transmission Electron Microscopy analysis confirmed tip-growth mechanism. Raman spectroscopy was used to map the patterned nanofibre arrays.


*Keywords:* Nanotubes; Nanofibers; Plasma CVD; Nanoparticles

## 1. Introduction

Carbon nanotubes (CNTs) and nanofibres (CNFs) are promising components for many applications, such as field emission devices, sensors, fuel cells, supercapacitors and batteries [1]. The design of nano-sized devices often involves patterns of carbon nanotubes or nanofibres firmly attached to the support [2]. The ability to grow vertically aligned nanotubes in patterns is an extra advantage or even a prerequisite for many applications including field emission devices such as electron sources for microwave amplifiers, X-ray tubes or ionisation detectors [3,4]. This process relies on the selective growth of nanotubes only where the catalyst is present. Dense mats of nanotubes can be grown by chemical vapour deposition (CVD) with vertical alignment due to their steric crowding [5,6]. However, a number of applications including field emission require arrays of well separated, free-standing nanotubes. A steric crowding mechanism will not provide alignment in that case.

Plasma Enhanced Chemical Vapour Deposition (PECVD), on the other hand, allows the direct growth of vertically aligned multiwalled nanotubes and nanofibres [2,7,8]. PECVD growth can be carried out at much wider range of temperatures down to low temperatures, inaccessible by standard thermal CVD [9–12]. The nanotubes are vertically aligned due to the growth in the electric field of the plasma sheath. CNTs grown in this way are generally multiwalled and, thus, robust enough to support themselves individually. Moreover, for electrochemical applications, stacked, herringbone or generally more defective CNFs offer a more active surface and possible intercalation between the graphene layers [13].

The accurate, large-scale 2D patterning of colloidal catalysts by conventional lithography is more difficult than sputtering or evaporation of thin films. CNT arrays have been fabricated using, for example, photolithography or micro-contact printing to pattern catalysts with 10 μm pattern feature sizes [14,15]. Alternatively, ink jet printing of cobalt colloid catalyst would allow the fabrication of nanotube patterns with comparable feature sizes [16]. Catalyst patterns have also been made by evaporation through shadow masks [17]. Finally, nano-imprint has been used to transfer polymethyl methacrylate (PMMA) masks [18], which are then used as a template for shadow masking.

We have recently reported nanocontact printing as an effective low-cost technique for patterning cobalt colloid catalyst for the fabrication of CNF arrays with sub-micron feature sizes [19,20]. In order to integrate such arrays into conventional

* Corresponding author. Fax: +44 1223 336362.
*E-mail address:* vbg20@cam.ac.uk (V.B. Golovko).

0925-9635/$ - see front matter © 2006 Elsevier B.V. All rights reserved.
doi:10.1016/j.diamond.2005.12.045

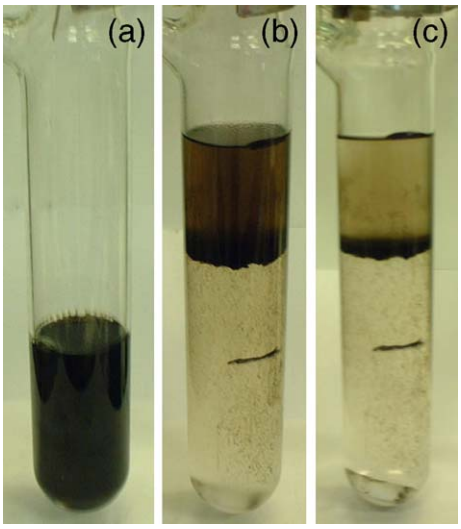


Fig. 1. Colloid purification by flocculation with methanol: (a) as synthesised colloid; (b) after 30 min of flocculation; (c) final layering after 3 h.

electronic devices it would be necessary to learn how to ensure a good electrical contact between the resulting nanotubes and metallised substrate [21]. We are currently developing a high-precision printing equipment allowing printing of colloid catalyst patterns over patterned metal substrates for the fabrication of addressable CNT arrays, which could be further integrated into electronic devices.

Here we present further results on the colloid synthesis, improved patterning, and the characterisation of our patterned arrays of vertically aligned carbon nanofibres by means of Scanning Electron Microscopy and Rutherford back-scattering detection, High Resolution Transmission Electron Microscopy and Raman spectroscopy. A reliable method is required for monitoring of quality of CNT array fabrication. Thus, we report on the results of Raman mapping of the as-grown samples for a qualitative assessment of the CNF patterns in terms of growth selectivity.

## 2. Experimental

Cobalt colloid was synthesised via the inverse micelle method using $CoCl_{2\ (aq)}$ and $NaBH_{4\ (aq)}$ micellar solutions in *iso*-octane stabilized by AOT (bis(2-ethylhexyl)sulfo succinate sodium salt). Reactants are divided into small micelles surrounded by molecules of surfactant and dispersed in inert organic solvent. On mixing, metal salt reduction is confined to the volume of collided micelles, with surfactant molecules prepositioned to stabilize produced metal particle. In order to remove an excess of surfactant required at the reduction stage, the cobalt colloid is then purified by flocculation (Fig. 1) with methanol according to the procedure reported by Raja et al. [22].

We have found that nanocontact printing required use of concentrated solutions of purified colloid as the ink. In a typical preparation, colloid made starting with 50 ml *iso*-octane, 6.0 g AOT, 1.2 ml of 0.3 M $CoCl_2$ and 0.6 M $NaBH_4$, respectively, was flocculated by 60 ml of methanol. The separated flocculated colloid was then re-dispersed in 10–20 ml of methanol. Additional filtration through 0.2 μm PTFE syringe filter and/or quick centrifugation was used to remove any large particle aggregates prior to printing. This allowed us to focus the particle size distribution in the colloid to a narrow range around 3.5 nm. Fig. 2 shows a High Resolution Transmission Electron Microscopy (HRTEM) JEOL 3010 (300 kV) images of the colloid confirming presence of monodisperse crystalline cobalt nanoparticles ~2–4 nm in diameter.

The nanocontact printing was performed using freshly prepared and purified cobalt colloid as ink. Poly-dimethyl siloxane (PDMS) stamps were fabricated with V-shaped lines or pyramids with sub-100 nm tip sizes and periodicity of 3–4 μm. The dot- and line-patterned stamps were made by replica moulding of Si masters fabricated by anisotropic etching or Focused Ion Beam (FIB) milling [23–25]. The line patterned V-shaped stamps were also made using commercially available silicon V-shaped 3 μm grating used for atomic force microscopy (AFM) tip characterization (TGG01 from MikroMashCo) as a master.

The PDMS stamp was cleaned by sonication in absolute ethanol, washing in water and blow-drying in nitrogen prior to each printing cycle. It was then inked with cobalt colloid and gently dried under $N_2$ flow. Silicon wafer substrates (~5 × 5 $mm^2$ size) were cleaned with acetone, absolute ethanol, and water. They were treated with a mild oxygen plasma prior to printing to improve their hydrophilicity [18]. The contact

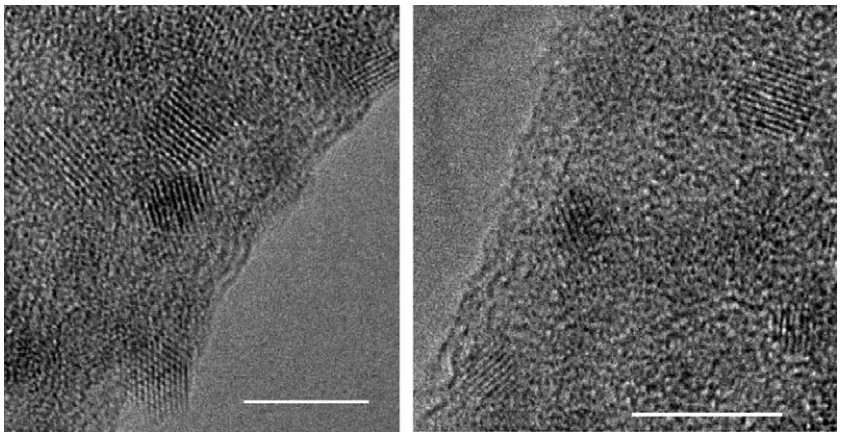

Fig. 2. HRTEM images showing individual colloidal nanoparticles. Scale bars: 5 nm.

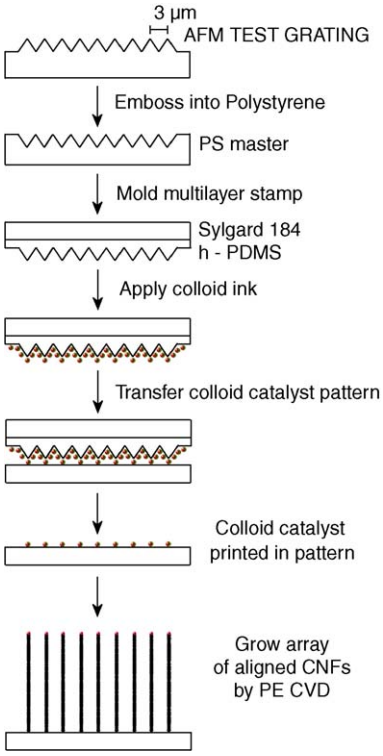


Fig. 3. Scheme of line-patterned CNF array fabrication.

between the dried stamp and cleaned silicon wafer was established manually (5–30 s), with care taken to ensure contact uniformity and avoid horizontal displacements. Fig. 3 summarises the overall process for the case of line-patterned CNF array fabrication. "As printed" samples were stored under Ar atmosphere prior to growth.

To perform CNF growth, "as-printed" samples were transferred into a DC PECVD vacuum chamber (background pressure $<10^{-6}$ mbar) and placed onto a resistively heated graphite block. A typical deposition process [10,11] involves a 15 min annealing in 200 sccm $NH_3$ flow (0.6 mbar) until the target growth temperature is reached. Plasma was then ignited by applying a 600 V DC discharge between the sample holder (cathode) and a gas inlet (anode) placed ~3 cm above it. $C_2H_2$ was then fed into the chamber through a side gas inlet for a total 50:200 sccm $C_2H_2$:$NH_3$ gas mixture (0.7 mbar). The gas mixture we used here was previously optimized to minimize any amorphous carbon deposition onto the un-patterned areas via $NH_3$ etching [8,10,26,27]. During a 30 min typical CNF deposition, the average plasma current was kept constant to 30–40 mA delivering a <20 W power. This ensures minimization of plasma heating effects.

The samples were characterized by Scanning Electron Microscopy (SEM, Jeol 6340 FEGSEM, LEO 1530VP FEGSEM), High Resolution Transmission Electron Microscopy (HRTEM, Jeol 3010, 300 kV) and Raman spectroscopy (Renishaw 1000 spectrometer, 514.5 nm laser excitation). For HRTEM analysis, the CNFs were removed from the substrates and dispersed onto holey carbon Cu TEM grids. In order to perform Raman mapping, the Raman spectrometer was coupled to a 200×200×20 μm excursion *XYZ* stage (Phyzik Instruments) capable of nanometer steps.

## 3. Results and discussion

We have successfully patterned arrays of lines and dots of colloidal catalyst by nanocontact printing with sub-micron resolution, and then grown patterned arrays of nanotubes by DC PECVD. Moreover, our high temperature growth results promise the ability to manufacture arrays with a single CNF per dot. The sub-100 nm pattern feature size is desired in this case, as it is previously shown that metal catalyst dots of such diameters can give arrays with only one nanotube per dot [7].

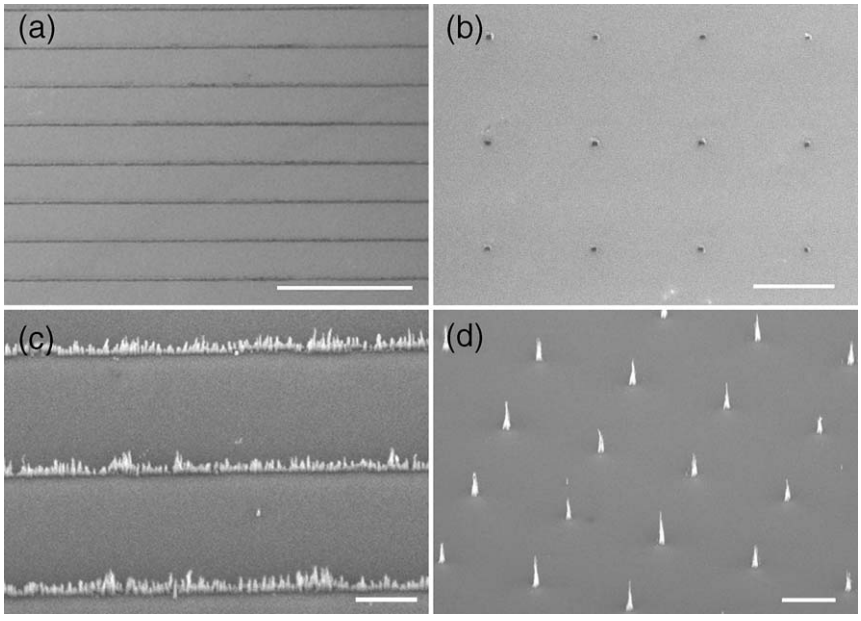


Fig. 4. SEM images of: cobalt colloid printed in (a) line- and (b) dot-patterns on silicon surface; carbon nanofibres grown in (c) line- and (d) dot-arrays at 640 and 510 °C, respectively. Scale bars: (a) 10 μm; (b) 1 μm; (c) 3 μm; (d) 2 μm.

SEM images of colloid catalyst printed onto silicon wafer surface shown in Fig. 4(a,b) confirm uniformity of pattern transfer by nanocontact printing over large substrate areas. These images provide an indication of the resolution achievable by nanocontact printing. Pattern feature sizes vary depending on the printing conditions, with feature sizes at 100 nm scale.

The catalyst behaviour during the pre-growth annealing is one of the crucial factors determining the type and quality of synthesized CNT/CNFs. In the case of thin films, heating in $NH_3$ atmosphere tends to restructure the metal catalyst into small islands. Coalescence triggers the coarsening of the film surface and its rearrangement in metal islands suitable to nucleate CNTs/CNFs [8,28]. Metal colloid precursors offer an advantage of pre-formed nano-sized particles with a chemically predefined diameter distribution. However, the pre-growth annealing causes nanoparticle aggregation and clustering due to sintering and Ostwald ripening effects [29,30]. Diameters of the as-grown CNTs/CNFs should correlate to the resulting metal catalyst particle sizes. This provides room for the growth process optimization required to fabricate arrays with a single CNT/CNF per printed catalyst dot.

Line- and dot-patterned nanotube arrays grown on silicon wafers using cobalt colloid catalyst are shown in Fig. 4(c,d), respectively. We see that thin, vertically aligned and similarly sized CNFs have grown directly on the surface. Fig. 4(c) shows that each line consists of a narrow row of CNFs, indicating that nanocontact printing can provide catalyst pattern feature sizes small enough to nucleate single, isolated CNFs. The sub-100 nm line width is achievable in a good case with typical line widths of 100–300 nm in other printing attempts with the same stamp. Fig. 5 shows that the feature sizes of the CNF arrays grown from colloid catalyst patterned using nanocontact printing and from e-beam patterned thin Co films are comparable. Fig. 4(d) shows SEM images of CNFs grown at ~500 °C from printed dot patterns of the colloids shown in Fig. 4(b). The figures

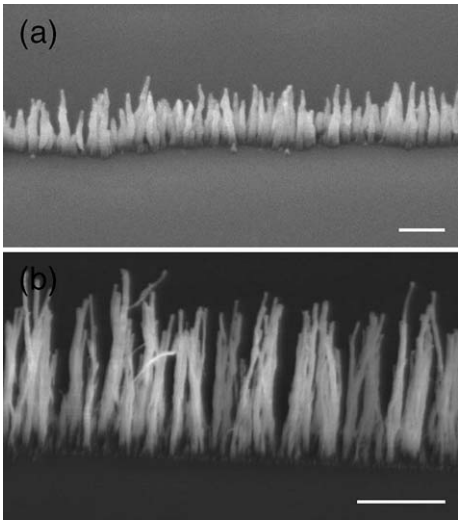


Fig. 5. SEM images of CNFs grown by DC PECVD from (a) cobalt colloid nanocontact-printed in lines at 640 °C and (b) from a 100 nm-wide, 5 nm-thick e-beam patterned cobalt metal catalyst line at ~550 °C. Scale bars: (a) 200 nm, (b) 1 μm.

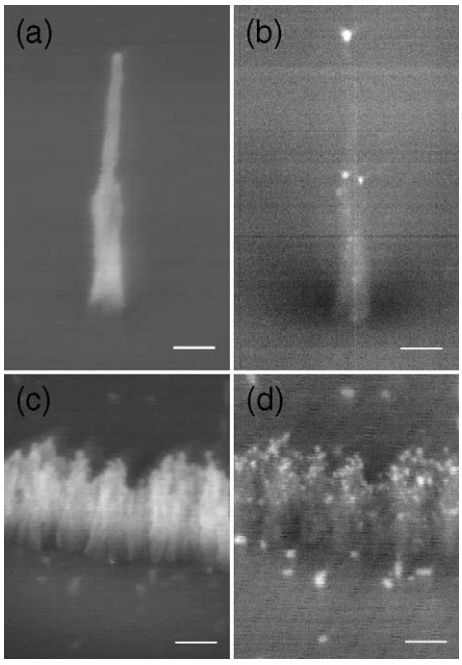


Fig. 6. (a, c) SEM and corresponding (b, d) RBS images of pattern fragments for dot- and line-patterned CNF arrays. Scale bars: 100 nm in all cases.

show that in most cases just a few nanofibres grow from each dot. Increased growth temperatures (>600 °C) could lead to the growth of a single CNF per dot due to the more pronounced sintering of catalyst nanoparticles into a larger droplet. This shows that the printing was able to achieve the resolution required to fabricate one nanofibre per dot arrays for above-mentioned applications.

Further characterisation of fabricated CNF arrays by direct non-destructive methods, confirmed tip-growth mechanism and selective nanofibre growth limited only to the areas covered by printed colloid catalyst. We have previously reported tip-growth mechanism for the vertically aligned nanofibres densely grown over large areas of silicon wafer substrates based on Transmission Electron Microscopy (TEM) analysis [9]. However, this required transfer of as-grown nanofibres from silicon wafer onto a holey carbon film supported on copper grid, commonly used in TEM analysis. Such method is destructive. Furthermore, it is cumbersome for samples containing relatively

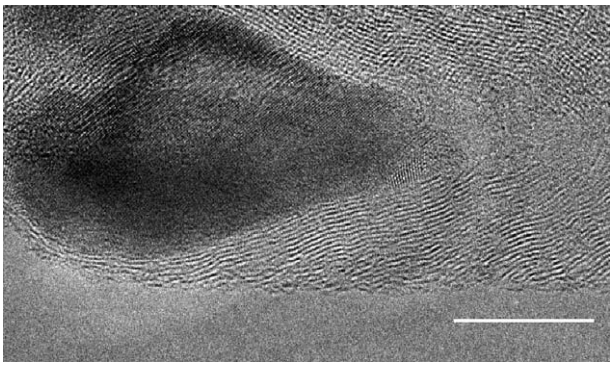

Fig. 7. HRTEM image of CNF tip (growth temperature: 450 °C). Scale bar: 10 nm.

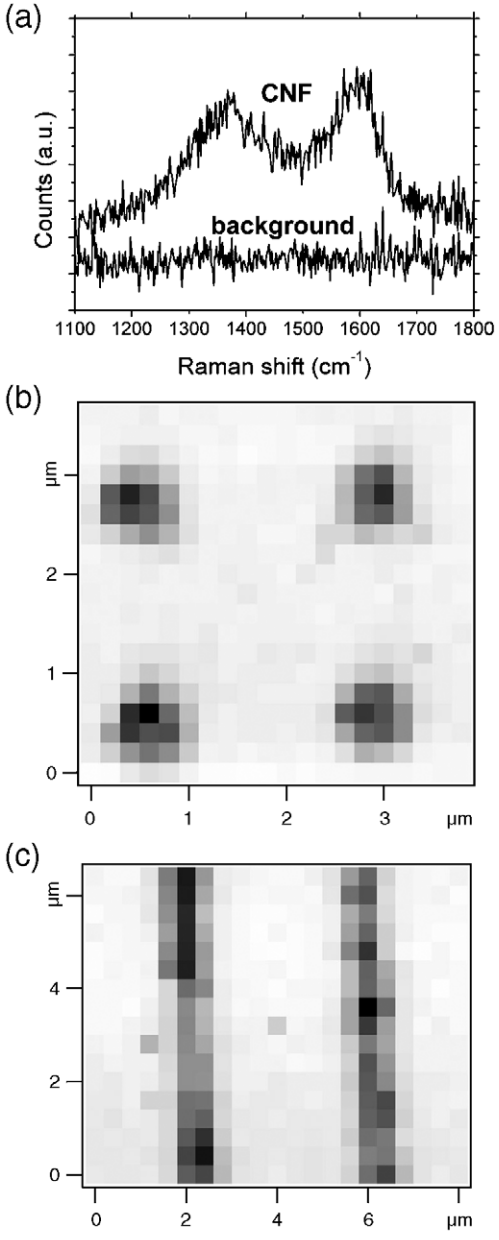


Fig. 8. (a) Raman spectra of vertically aligned CNFs grown at 450 °C, and Raman maps of (b) dot- (200 nm scan step) and (c) line-patterned (400 nm scan step) arrays. Raman maps are acquired integrating the Raman signal in the 1200–1700 $cm^{-1}$ spectral region.

few nanofibres, such as patterned nanofibre arrays reported here. Therefore, a direct and preferably non-destructive method is required in order to determine the growth mechanism. Scanning Electron Microscopy analysis using Rutherford back-scattering (RBS) detection is ideal for this purpose. RBS has better sensitivity in the detection of elements with higher atomic numbers, and thus it enhances the image contrast among the different elements present in a sample in comparison with conventional SEM secondary-electron imaging. SEM and corresponding RBS images clearly show that cobalt catalyst nanoparticles are located in the CNF tips in the case of dot- and line-patterned arrays (Fig. 6). TEM analysis (Fig. 7), despite mentioned above difficulty in sample preparation, provides additional confirmation of the tip-growth mechanism. Thus, tip growth mechanism can be postulated for the reported here arrays of vertically aligned nanofibres DC PECVD grown using cobalt colloid catalyst nanocontact printed on silicon substrate. Tip growth mechanism ensures vertical alignment due to the compensatory effect of plasma electromagnetic field [31]. HRTEM image (Fig. 7) also shows the crystalline quality of the grown CNFs with a structure intermediate between herring-bone and bamboo-like. The highly crystalline cobalt particle at the CNF tip is much larger than the original colloid nanoparticles (Fig. 2) due the sintering during annealing stage.

We assessed the uniformity and chemical selectivity of our line- and dot-patterned arrays of vertically aligned CNFs by Raman mapping. This technique has been successfully used in the past to locate selected, individual CNT bundles and even single CNTs in far-field [32,33] and near-field configurations [34]. In the far-field case, sub-micron resolution is achieved even if the laser spot size is larger than the used scanning steps. Fig. 8(a) shows a Raman spectrum representative of the CNF arrays in Fig. 8(b,c). The G-peak is due to the bond stretching of all pairs of $sp^2$ atoms in both rings and chains [35]. The D-peak is due to the breathing modes of $sp^2$ atoms in rings [35]. There is no radial breathing mode because the CNFs are >>5 nm in diameter and they are not single-walled. The selectivity of our growth process is demonstrated in Fig. 8(b,c). They show Raman maps of the dot- and line-patterned samples, acquired integrating the Raman signal in the 1200–1700 $cm^{-1}$ spectral region, and scanning the samples with steps of 200 and 400 nm, respectively. No carbon signal is detected outside the patterned area, as shown in Fig. 8(a). This implies a highly selective CNF growth with no deposition of amorphous carbon or other carbon nanostructures between the colloid patterned areas. Such selectivity is important for both field emission and electro-chemical applications.

## 4. Conclusions

We successfully used nanocontact printing to pattern cobalt colloid over large areas for the selective growth of vertically aligned carbon nanofibre arrays (lines and dots). The preparation of the colloid ink is described. The tip growth mechanism was postulated using Scanning Electron Microscopy analysis with Rutherford back-scattering detection and confirmed by Transmission Electron Microscopy analysis. A novel approach to pattern mapping was developed using Raman spectroscopy. Raman maps obtained clearly show selective nanofibre growth only over catalyst pattern.

## Acknowledgements

This work was supported by the EU project CARDECOM GRD1-2001-41830. We thank H.W. Li, Z. Yang and W.T.S. Huck for providing stamps and assisting with nanocontact printing. We thank Mr. D. Nicol and Mr. D. Vowles for assistance with the SEM. S.H. thanks Peterhouse College, Cambridge for Research Fellowship. A.C.F. acknowledges funding from the Royal Society.

## References


[1] H. Dai, Acc. Chem. Res. 35 (2002) 1035.
[2] A.V. Melechko, V.I. Merkulov, T.E. McKnight, M.A. Guillorn, K.L. Klein, D.H. Lowndes, M.L. Simpson, J. Appl. Phys. 97 (2005) 041301.
[3] W.I. Milne, K.B.K. Teo, G.A.J. Amaratunga, P. Legagneux, L. Gangloff, J.P. Schnell, V. Semet, V.T. Binh, O. Groening, J. Mater. Chem. 14 (2004) 933.
[4] K.B.K. Teo, E. Minoux, L. Hudanski, F. Peauger, J.P. Schnell, L. Gangloff, P. Legagneux, D. Dieumegard, G.A.J. Amaratunga, W.I. Milne, Nature 437 (2005) 968.
[5] K. Hata, D.N. Futaba, K. Mizuno, T. Namai, M. Yumura, S. Ijima, Science 306 (2004) 1362.
[6] S.S. Fan, M.G. Chapline, N.R. Franklin, T.W. Tombler, A.M. Cassell, H.J. Dai, Science 283 (1999) 512.
[7] K.B.K. Teo, S.B. Lee, M. Chhowalla, V. Semet, V.T. Binh, O. Groening, M. Castignolles, A. Loiseau, G. Pirio, P. Legagneux, D. Pribat, D.G. Hasko, H. Ahmed, G.A.J. Amaratunga, W.I. Milne, Nanotechnology 14 (2003) 204.
[8] M. Chhowalla, K.B.K. Teo, C. Ducati, N.L. Rupesinghe, G.A.J. Amaratunga, A.C. Ferrari, D. Roy, J. Robertson, W.I. Milne, J. Appl. Phys. 90 (2001) 5308.
[9] B. Kleinsorge, V.B. Golovko, S. Hofmann, J. Geng, D. Jefferson, J. Robertson, B.F.G. Johnson, Chem. Commun. 12 (2004) 1416.
[10] S. Hofmann, C. Ducati, J. Robertson, B. Kleinsorge, Appl. Phys. Lett. 83 (2003) 135.
[11] S. Hofmann, C. Ducati, B. Kleinsorge, J. Robertson, Appl. Phys. Lett. 83 (2003) 4661.
[12] S. Hofmann, G. Csanyi, A.C. Ferrari, M.C. Payne, J. Robertson, Phys. Rev. Lett. 95 (2005) 036101.
[13] M. Endo, Y.A. Kim, T. Hayashi, K. Nishimura, T. Matusita, K. Miyashita, M.S. Dresselhaus, Carbon 39 (2001) 1287.
[14] H. Kind, J.M. Bonard, L. Forro, K. Kern, K. Hernadi, L.O. Nilsson, L. Schlapbach, Langmuir 16 (2000) 6877.
[15] S. Huanga, A.H.W. Mau, Appl. Phys. Lett. 82 (2003) 796.
[16] H. Ago, K. Murata, M. Yumura, J. Yotani, S. Uemura, Appl. Phys. Lett. 82 (2003) 811.
[17] Z.P. Huang, D.L. Carnahan, J. Rybczynski, M. Giersig, M. Sennett, D.Z. Wang, J.G. Wen, K. Kempa, Z.F. Ren, Appl. Phys. Lett. 82 (2003) 460.
[18] S.M.C. Vieira, L.T. Gangloff, O. Groening, K.B.K. Teo, E. Minoux, P. Legagneux, P. Andrew, G.A.J. Amaratunga, W.I. Milne, Nanolett. (in press).
[19] V.B. Golovko, H.W. Li, B. Kleinsorge, S. Hofmann, J. Geng, M. Cantoro, Z. Yang, D.A. Jefferson, B.F.G. Johnson, W.T.S. Huck, J. Robertson, Nanotechnology 16 (2005) 1636.
[20] S. Hofmann, M. Cantoro, M. Kaempgen, D.J. Kang, V.B. Golovko, H.W. Li, Z. Yang, J. Geng, W.T.S. Huck, B.F.G. Johnson, S. Roth, J. Robertson, Appl. Phys., A 81 (2005) 1559.
[21] J. Moser, R. Panepucci, Z.P. Huang, W.Z. Li, Z.F. Ren, A. Usheva, M.J. Naughton, J. Vac. Sci. Technol., B 21 (2003) 1004.
[22] R. Raja, V.B. Golovko, J.M. Thomas, A. Berenguer-Murcia, W. Zhou, S. Xie, B.F.G. Johnson, Chem. Commun. 15 (2005) 2026.
[23] H.W. Li, B.V.O. Muir, G. Fichet, W.T.S. Huck, Langmuir 19 (2003) 1963.
[24] Y.N. Xia, G.M. Whitesides, Adv. Mater. 8 (1996) 765.
[25] H.W. Li, D.J. Kang, M.G. Blamire, W.T.S. Huck, Nanotechnology 14 (2003) 220.
[26] K.B.K. Teo, M. Chhowalla, G.A.J. Amaratunga, W.I. Milne, D.G. Hasko, G. Pirio, P. Legagneux, F. Wyczisk, D. Pribat, Appl. Phys. Lett. 79 (2001) 1534.
[27] M.S. Bell, R.G. Lacerda, K.B.K. Teo, N.L. Rupesinghe, G.A.J. Amaratunga, W.I. Milne, M. Chhowalla, Appl. Phys. Lett. 85 (2004) 1137.
[28] S. Hofmann, M. Cantoro, B. Kleinsorge, C. Casiraghi, A. Parvez, J. Robertson, C. Ducati, J. Appl. Phys. 98 (2005) 034308.
[29] J.M. Wen, J.W. Evans, M.C. Bartelt, J.W. Burnett, P.A. Thiel, Phys. Rev. Lett. 76 (1996) 652.
[30] N.C. Bartelt, W. Theis, R.M. Tromp, Phys. Rev., B 54 (1996) 11741.
[31] V.I. Merkulov, A.V. Melechko, M.A. Guillorn, D.H. Lowndes, M.L. Simpson, Appl. Phys. Lett. 79 (2005) 2970.
[32] F.K.A. Mews, T. Basché, G. Philipp, G.S. Duesberg, S. Roth, M. Burghard, Adv. Mater. 12 (2000) 1210.
[33] C.Y. Jiang, J.L. Zhao, H.A. Therese, M. Friedrich, A. Mews, J. Phys. Chem., B 107 (2003) 8742.
[34] A. Hartschuh, E.J. Sanchez, X.S. Xie, L. Novotny, Phys. Rev. Lett. 90 (2003) 095503-1.
[35] A.C. Ferrari, J. Robertson, Phys. Rev., B 61 (2000) 14095.